AIP | Biomicrofluidics
Fundamentals, Perspectives & Applications
#1 ORIGINAL RESEARCH FLUIDS JOURNAL IN THE FLUID AND PLASMA PHYSICS CATEGORY

Polyester μ-assay chip for stem cell studies

Francesco Piraino, Šeila Selimović, Marco Adamo, Alessandro Pero, Sam Manoucheri, Sang Bok Kim, Danilo Demarchi, and Ali Khademhosseini

Citation: Biomicrofluidics **6**, 044109 (2012); doi: 10.1063/1.4766300
View online: http://dx.doi.org/10.1063/1.4766300
View Table of Contents: http://scitation.aip.org/content/aip/journal/bmf/6/4?ver=pdfcov
Published by the AIP Publishing

Articles you may be interested in

Interaction between drug delivery vehicles and cells under the effect of shear stress
Biomicrofluidics **9**, 052605 (2015); 10.1063/1.4923324

Experimental demonstration of bindingless signal delivery in human cells via microfluidics
J. Appl. Phys. **116**, 044702 (2014); 10.1063/1.4891017

A polystyrene-based microfluidic device with three-dimensional interconnected microporous walls for perfusion cell culture
Biomicrofluidics **8**, 046505 (2014); 10.1063/1.4894409

An integrated microfluidic cell array for apoptosis and proliferation analysis induction of breast cancer cells
Biomicrofluidics **4**, 044104 (2010); 10.1063/1.3497376

Herceptin functionalized microfluidic polydimethylsiloxane devices for the capture of human epidermal growth factor receptor 2 positive circulating breast cancer cells
Biomicrofluidics **4**, 032205 (2010); 10.1063/1.3480573

Did your publisher get
18 MILLION DOWNLOADS in 2014?
AIP Publishing did.

AIP Publishing THERE'S POWER IN NUMBERS. Reach the world with AIP Publishing.

This article is copyrighted as indicated in the article. Reuse of AIP content is subject to the terms at: http://scitation.aip.org/termsconditions. Downloaded to IP: 18.7.29.240 On: Wed, 19 Aug 2015 20:51:52

Polyester μ-assay chip for stem cell studies

Francesco Piraino,[1,2,3,a)] Šeila Selimović,[2,3,a)] Marco Adamo,[2,3,4] Alessandro Pero,[2,3,4] Sam Manoucheri,[2,3] Sang Bok Kim,[2,3] Danilo Demarchi,[4] and Ali Khademhosseini[2,3,5,b)]

[1]*Bioengineering Department, Politecnico di Milano, Piazza Leonardo da Vinci 32, 20133 Milano, Italy*
[2]*Center for Biomedical Engineering, Department of Medicine, Brigham and Women's Hospital, Harvard Medical School, Cambridge, Massachusetts 02139, USA*
[3]*Harvard-MIT Division of Health Sciences and Technology, Massachusetts Institute of Technology, Cambridge, Massachusetts 02139, USA*
[4]*Politecnico di Torino, Department of Electronics and Communications, 10129 Torino, Italy*
[5]*Wyss Institute for Biologically Inspired Engineering, Harvard University, Boston, Massachusetts 02115, USA*

(Received 20 August 2012; accepted 23 October 2012; published online 26 November 2012)

The application of microfluidic technologies to stem cell research is of great interest to biologists and bioengineers. This is chiefly due to the intricate ability to control the cellular environment, the reduction of reagent volume, experimentation time and cost, and the high-throughput screening capabilities of microscale devices. Despite this importance, a simple-to-use microfluidic platform for studying the effects of growth factors on stem cell differentiation has not yet emerged. With this consideration, we have designed and characterized a microfluidic device that is easy to fabricate and operate, yet contains several functional elements. Our device is a simple polyester-based microfluidic chip capable of simultaneously screening multiple independent stem cell culture conditions. Generated by laser ablation and stacking of multiple layers of polyester film, this device integrates a 10×10 microwell array for cell culture with a continuous perfusion system and a non-linear concentration gradient generator. We performed numerical calculations to predict the gradient formation and calculate the shear stress acting on the cells inside the device. The device operation was validated by culturing murine embryonic stem cells inside the microwells for 5 days. Furthermore, we showed the ability to maintain the pluripotency of stem cell aggregates in response to concentrations of leukemia inhibitory factor ranging from 0 to ~1000 U/ml. Given its simplicity, fast manufacturing method, scalability, and the cell-compatible nature of the device, it may be a useful platform for long-term stem cell culture and studies. © *2012 American Institute of Physics*. [http://dx.doi.org/10.1063/1.4766300]

INTRODUCTION

An important challenge in the field of bioengineering is to engineer tissues for transplantation or drug discovery applications. Here, the research efforts often utilize stem cells for differentiation into various other cell types, such as endothelial cells,[1,2] cardiomyocytes,[3–6] or hepatocytes.[7–9] To better understand the differentiation process, many stimuli present in the native cellular microenvironment are explored in the laboratory, in particular, chemical cues. Among the well-known growth and differentiation factors affecting stem cell behavior are vascular endothelial growth factor (VEGF),[10] retinoic acid,[11] fibroblast growth factor (FGF-2),[12] and bone morphogenetic protein (BMP-2).[13]

[a)]F. Piraino and Š. Selimović contributed equally to this work.
[b)]Author to whom correspondence should be addressed. Email: alik@rics.bwh.harvard.edu. Fax: + 1 617 768 8477.

 © 2012 American Institute of Physics

This article is copyrighted as indicated in the article. Reuse of AIP content is subject to the terms at: http://scitation.aip.org/termsconditions. Downloaded to IP: 18.7.29.240 On: Wed, 19 Aug 2015 20:51:52

Simultaneous testing of a large number of chemical cues in stem cell applications may be possible using microscale platforms, which operate on microfluidic principles.[14–17] Aside from cost- and time-efficiency of microfluidic experiments, the appeal of this microscale technology comes from the ability to quickly generate precisely controlled, stable, and spatially varying mixtures of chemical reagents and biological samples.[18–20] Thus, microfluidic devices like the platform we present in this paper can offer precise control over the type and concentration of chemical cues in the cellular microenvironment. Such microfluidics-based concentration gradient devices can generally be separated into passive (diffusive) and active (convection based) gradient generators (GG).[21] Among the diffusion-based GGs are the so-called tree-like GG[22] and the Universal GG,[23] both of which are capable of generating a variety of concentration profiles from only two aqueous input solutions. Other structures that utilize passive mixing via diffusion can give rise to logarithmic,[24] sigmoidal,[25] and exponential[26] gradients, as is the case here, as well as combinatorial solution mixtures.[27] A special type of a diffusion-based mixing unit is the rotary mixer. It consists of a toroidal channel, into which several liquids are introduced one after another, and pumped using microvalves.[28] Here, each solution has a parabolic Poiseuille flow profile, and a mixing interface is generated orthogonally to the flow direction. Convective mixing[29] is another mechanism that can be utilized in microfluidic devices for generation of concentration gradients. For example, solutions flowing through curved channels[30] experience eddies at points with the largest radii of curvature and are mixed chaotically. Ratchet structures, investigated by Stroock and McGraw, Whitesides[31] and Yager[32] groups, function in a similar manner. When a sheet of liquid passes over angled ratchets on the bottom of a microfluidic channel,[33] it experiences a pressure gradient that drives it back across the channel ceiling. The liquid effectively folds upon itself, and particles present in different parts of the flow mix with each other. Both GG types have impacted a wide range of biological studies, including cancer metastasis, immune response, angiogenesis, and others.[34–36] In addition, microfluidic GGs have been used to investigate stem cell behavior,[24] e.g., the influence of a mixture of growth factors on human neural stem cell proliferation and differentiation[12] and the effect of a bovine serum albumin concentration gradient on human embryonic stem cell viability and morphology.[37]

Despite the variety of microfluidic devices for stem cell applications,[17] there is a dearth of simple-to-use, yet potentially powerful experimental platforms with the capability to test cellular response to a chemical concentration gradient. This is due to the breadth of engineering approaches, most of which utilize one of two opposing strategies. Either the experimental platforms are designed to carry out several functions simultaneously, which makes them cumbersome to fabricate and difficult to operate, or the devices are architecturally simple and easy to use, but lack complex functionalities.[15,38] In the first case, the goal is to create a highly controlled stem cell microenvironment and conduct high-throughput screening of differentiation cues. Thus, microfluidic valves and multiplexers are often incorporated into the devices for gradient and flow control, as shown by Mosadegh *et al.*[39] and Gomez-Sjoberg *et al.*,[40] which requires a high level of technical skill and potentially a programmable interface for automated operation. Similarly, Kim *et al.*[41] enabled controlled on-chip cell loading, delivery of a range of chemical growth factors and immunostaining at the expense of a complicated 3-layer master mold fabrication, and the inclusion of externally driven microvalves. In the second case, microfluidic devices for stem cell studies tend to be confined to either single-cell trapping, culture and analysis[42] or to growth of embryonic bodies in individual microwells.[43–45] These platforms have no more than one or two fluidic layers and contain a perfusion channel superposed onto a microwell array. They are also low-throughput, as they generally supply few different, manually prepared chemical solutions to the captured cells.[46] For example, Liu *et al.*[47] developed a simple microscale platform combining channels and wells with different substrates for stem cell culture and differentiation, but did not incorporate further functionalities such as screening against different growth factors. Toh *et al.*[48] initially also chose a simple microfluidic structure consisting of three culture and perfusion channels for 3D stem cell culture that could be used to observe the cell proliferation and differentiation behavior in response to a single chemical factor. Later, they extended the platform to include a linear concentration gradient generator, but the testing was confined to a liver cancer cell line.[49]

This article is copyrighted as indicated in the article. Reuse of AIP content is subject to the terms at: http://scitation.aip.org/termsconditions. Downloaded to IP: 18.7.29.240 On: Wed, 19 Aug 2015 20:51:52

To introduce a user-friendly, yet potentially powerful microfluidic stem cell culture and differentiation device, we have extended our polyester-based cell culture platform to include a microfluidic continuous perfusion system and a concentration gradient generator, without having to sacrifice the simplicity of the fabrication technique. We have previously shown that microwell platforms could be easily and quickly manufactured using laser ablation of sticky polyester films.[50] Furthermore, we demonstrated that this material could be used in cell experiments without deleterious effects on the cell viability. The polyester μ-assay chip presented here combines microwells for cell storage and 3D culture with a network of microfluidic channels. This network serves as a delivery path for cells, functions as a continuous cell perfusion system, and is used to form and transport to the stored cells several on-chip prepared concentrations of chemical factors. This is accomplished in the form of nonlinear concentration gradients. In this paper, we demonstrate the utility of the polyester μ-assay chip for stem cell culture. As a validation test, we study the effect of an imposed exponential gradient of leukemia inhibitory factor (LIF) on the expression of a fluorescent indicator of Oct4, a transcription factor regulated in pluripotent stem cells.

MATERIALS AND METHODS

Device fabrication

The polyester film used to fabricate the microfluidic device was provided by adhesive applications (NT 8512-2DL; Easthampton, MA). It consisted of a central 50.8 μm thick polyester layer and 38.1 μm thick layers of silicone glue on both sides. Each glue layer was protected with a 50.8 μm thick polyester liner (Figure 1(a)). The well layer of the device was patterned by laser ablation of the polyester film, as described elsewhere,[50] in order to yield a 10×10 array of 150 μm large circular microwells with a conical cross-section. The laser power chosen was 3.6 W and the printing speed was 22.9 cm/s. The height of the microwells was 178 μm,

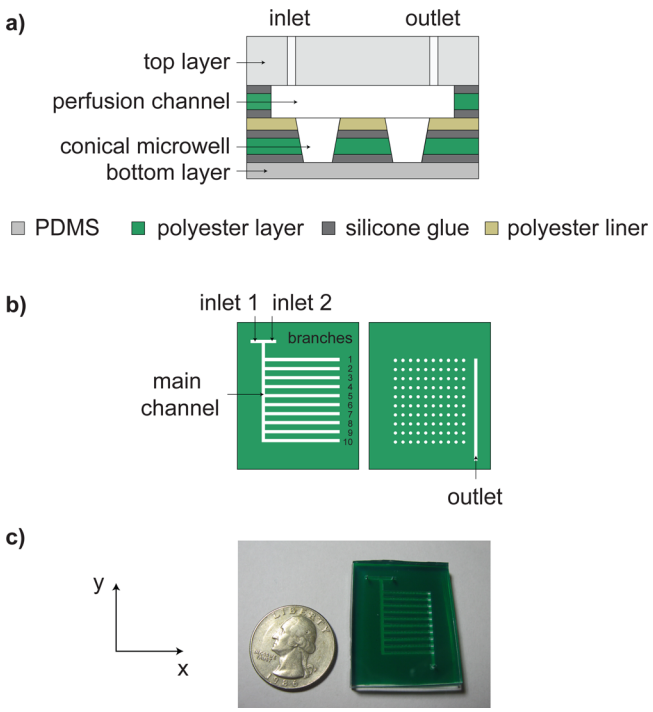

FIG. 1. Schematic of the polyester μ-assay chip. (a) The device cross-section shows four layers (a top PDMS layer, a polyester layer containing fluidic channels, a polyester layer containing microwells, and a bottom PDMS layer), which were aligned and bonded utilizing the silicon glue on the polyester film. (b) Schematic of the channels and the well layers (top view). The branches 1–10 were superposed onto different rows of microwells. (c) Photograph of the assembled device.

This article is copyrighted as indicated in the article. Reuse of AIP content is subject to the terms at: http://scitation.aip.org/termsconditions. Downloaded to IP: 18.7.29.240 On: Wed, 19 Aug 2015 20:51:52

resulting in a well volume of 11.6 nl. The wells were placed 1 mm along the x-direction, and 2 mm along the y-direction, as defined in Figure 1. The well layer also contained the output channel (1 mm wide, 23 mm long). A second polyester film was patterned with additional fluidic channels (Figure 1(b)). The 10 channel branches were 800 μm wide, while the main channel was 1 mm wide and 23 mm long. The height of these channels was 127 μm, less than the microwell height because the top polyester liner was removed. All channels were printed at 1.5 W and 5.72 cm/s.

The two polyester layers were aligned manually on an inverted microscope, such that each channel branch was superposed onto a row of 10 microwells (Figure 1(a)). The sticky film surface was utilized to subsequently glue the polyester structure to a blank, 1 mm thick slab of poly(dimethylsiloxane) (PDMS, Sylgard 184; Dow Corning, Midland, MI), which formed the bottom of the microwells. Then, the assembled structure was treated with oxygen plasma (Harrick Plasma, Ithaca, NY) for 20 s at 18 W, which temporarily rendered the polyester film hydrophilic (see supplementary material, Figure S-1).[51] Finally, a 4 mm thick PDMS layer was glued on top of the channels. This layer contained input and output ports for fluidic connections, carved with a sharpened 23 G needle. Any air bubbles trapped between the layers during the device assembly were removed by applying uniform pressure to the device and allowing the bubbles to diffuse into the PDMS layers. The completed device is shown in Figure 1(c).

Numerical calculation and computational fluid dynamics simulations

We developed two numerical models employing the commercial solvers COMSOL MULTIPHYSICS (COMSOL, Burlington, MA) and CFD-ACE+ 2004.0.25 (ESI-CFD Inc., Huntsville, AL). First, we created a two-dimensional COMSOL model to determine the optimal channel network geometry, which would enable the generation of long-term stable, non-linear concentration gradients of an analyte, such as rhodamine B or fluorescein isothiocyanate (FITC), in water. The working mechanism of the gradient generation was discussed in detail elsewhere.[25] Assuming isothermal, steady-state, laminar, and uniaxial fluid flow inside the device, the following governing equations were identified:

$$\nabla P - \mu \nabla^2 u = 0 \,(\text{Navier} - \text{Stokes}), \tag{1}$$

$$\nabla \cdot u = 0 \,(\text{Continuity}), \tag{2}$$

$$u \nabla c = D \nabla^2 c \,(\text{Transport}), \tag{3}$$

where $\boldsymbol{u}$ is the velocity vector, P is the pressure, and c is the analyte concentration. The model required the following parameters: dynamic viscosity (μ) of water (10^{-3} Pa s), hydraulic diameter (d) of the main channel (225 μm), mass diffusivity (D) of the analyte (3.6×10^{-10} m^2/s for rhodamine B[23] and 4.9×10^{-10} m^2/s for FITC),[24] and initial analyte concentration (c_0) (0.03% w/v for rhodamine B and 0.02% w/v for FITC). In addition, we varied the values for the applied flow rate at each of the two inlets (Q), and the corresponding average velocity ($\bar{U}$) inside the main channel: for $Q = 10$ μl/h, $\bar{U} = 24.3$ μm/s; for $Q = 50$ μl/h, $\bar{U} = 121.5$ μm/s; and for $Q = 200$ μl/h, $\bar{U} = 486$ μm/s. Equations (1) and (2) were approximated computationally to determine the fluid flow field and Eq. (3) was used to determine the concentration distribution of the analyte. We compared our numerical results with the analytical solution of Fick's law and optimized the discretization parameters using unstructured triangular mesh elements ranging from 4 μm to 40 μm in size (0.5% and 5% of the main channel width, respectively). The boundary conditions (BCs) at the main channel inlet were: $Q_1 = Q_2 = Q$; $c_1 = 0$; $c_2 = 1$, where Q_1 and Q_2 are the inlet flow rates [μl/h] for the analyte solution and pure water, and c_1 and c_2 are the normalized inlet concentrations of dye in the pure water and dye solutions. Next, we imposed no slip and Neumann BCs at the channel walls ($\boldsymbol{u} = 0$, $\partial c/\partial n = 0$), as well as a zero pressure condition and Neumann BCs at the channel outlet ($P = 0$; $\partial c/\partial n = 0$).

Second, we utilized the CFD-ACE+ solver to calculate the shear stress near the microwells and add to our observations of cells inside the device. We developed a three-dimensional

This article is copyrighted as indicated in the article. Reuse of AIP content is subject to the terms at: http://scitation.aip.org/termsconditions. Downloaded to IP: 18.7.29.240 On: Wed, 19 Aug 2015 20:51:52

transient-state model of the volume surrounding a single microwell, discretized with tetragonal elements in an unstructured mesh. Because of the symmetry of the problem, we only had to model one half of a microwell. The governing equations under the same hypothesis discussed above were Eq. (2) and the following:

$$\tau = -\mu\gamma \,(\text{Shear stress}) \tag{4}$$

where $\boldsymbol{g}$ is the gravitational acceleration, τ is the shear stress, and γ is the shear rate. The values for the dynamic viscosity (μ) and density (ρ) of the cell culture medium were 0.78×10^{-3} Pa s and 990 kg/m^3, respectively.[25] We calculated the shear stress acting on the cells inside the device for different experimental conditions. For example, cells would be introduced into the device through the output channel at a concentration of 10^6 cells/ml and a flow rate of $Q_{cell} = 7200\ \mu$l/h, but the highest flow rate used for the gradient generation would be $Q = 200\ \mu$l/h per input stream. We modeled the cells as elastic spherical particles with Young's modulus of 1 kPa, a density of 1100 kg/m^3,[26] and diameters ranging from 5 μm to 25 μm. The applied BC at the top of the microwell was $\bar{U}_{in} = \bar{U}_0$. Because the microwells were located inside one of the 10 channel branches, the average flow rates and velocity were $Q_{cell} = 7200\ \mu$l/s ($\bar{U}_0 = 1.749$ mm/s) and $Q = 200\ \mu$l/h ($\bar{U}_0 = 486\ \mu$m/s). We also applied no slip BCs at all microwell walls ($\boldsymbol{u} = 0$), a Neumann BC along the conduit center line ($\partial u/\partial n = 0$), and a zero pressure BC at the channel outlet ($P = 0$).

Concentration gradient

We validated experimentally the numerical prognosis of dye concentration gradients by forming different non-linear gradients of fluorescent dye in water. We injected pure water into the device through inlet 1 and a fluorescent dye solution through inlet 2 using gas-tight glass syringes (008425; SGE, Austin, TX) at equal flow rates. We used a programmable syringe pump (Harvard PhD 2000; Harvard Apparatus, Holliston, MA) to control the individual flow rates of the two solutions (10 μl/h, 50 μl/h, and 200 μl/h) and generate different concentration gradients. At each flow rate, we waited until the device was completely filled and all air bubbles were removed. Then, we waited for 20 min before observing the dye distribution in the device, in order to ensure that the concentration gradient had reached steady state. We recorded fluorescence images of all wells using a Nikon Eclipse TE2000 microscope with a 2× objective. In our experiments on rhodamine B (0.03% w/v in water) and FITC (0.02% w/v in water), we measured the mean intensity of the dye over the area of each well, using IMAGEJ software (http://rsbweb.nih.gov/ij/). We hypothesized, in accordance with published literature,[52,53] that for low dye concentrations the dye intensity was proportional to the dye concentration.

Murine embryonic stem cell (mESC) culture

We obtained all tissue culture components from the Gibco-Invitrogen Corporation (Grand Island, NY), unless specified otherwise. Genetically engineered mESCs expressing green fluorescent protein (GFP) upon expression of Oct4 promoter were first cultured in ESC medium containing high glucose-Dulbecco's modified eagles medium (DMEM), enriched with 10% v/v ES qualified FBS, 100 mg/ml streptomycin, 100 U/ml penicillin, 1% v/v nonessential amino acid solution, 0.1 mM b-mercaptoethanol, 1 mM L-glutamine, and 0.1% of 10^6 U/ml leukemia inhibitory factor (ESG1107; Millipore, Billerica, MA). For the on-chip culture experiments, we used minimal essential medium (α-MEM) to promote cell aggregation, enriched with 15% (v/v) heat inactivated-fetal bovine serum (HI-FBS), 100 mg/ml streptomycin, and 100 U/ml penicillin.

Cell loading, aggregate formation, and viability

The device was sterilized under UV light for 5 min and was filled from the outlet with sterile PBS immediately after fabrication. At this time, the polyester film was still hydrophilic, allowing us to remove air trapped inside the microwells. We waited for 45 min until the polyester had

This article is copyrighted as indicated in the article. Reuse of AIP content is subject to the terms at: http://scitation.aip.org/termsconditions. Downloaded to IP: 18.7.29.240 On: Wed, 19 Aug 2015 20:51:52

relaxed back to its hydrophobic state[54] and introduced cell culture medium into the device. Then, the cells were suspended in 20 μl of medium at a concentration of 10^6 cells/ml and introduced into the device through the outlet channel, using a 3 ml plastic syringe (Becton-Dickinson, NJ, USA), similar to the method of Liu *et al.*[47] The device was visually inspected under the microscope to ensure uniform cell distribution. Then, the flow was stopped for 5 min, allowing the cells to sink to the bottom of the channels and wells, as shown previously.[55,56] Last, we washed away the cells that had settled on the bottom of the channels by infusing culture medium from the outlet. At this step, the flow was controlled using a programmable syringe pump (Harvard PhD 2000; Harvard Apparatus, Holliston, MA), at a rate of 300 μl/h.

Once loaded with cells, the devices were kept inside a cell culture incubator, with culture medium flowing continuously for 5 days at a total flow rate of 400 μl/h. The mESCs started aggregating inside the polyester microwells within one day of culture. We recorded daily phase contrast images of all microwells. We used the IMAGEJ Area function to measure the area of each cell aggregate large enough to be observed. The minimum resolution was 20 μm. The average was calculated across a total of 300 wells on 3 separate devices. A viability test was conducted on day 5 by a calcein-AM/ethidium homodimer live/dead assay (Invitrogen). Cells were washed with Dulbecco's phosphate-buffered saline (DPBS), followed by 50 μl of 2 mM calcein-AM and 4 mM ethidium homodimer in DPBS. Samples were incubated for 20 min, then washed once with DPBS and finally imaged at 2× and 4×.

Stem cell pluripotency

LIF was added to the culture medium to prevent loss of mESC pluripotency inside the microwells. This relationship between LIF and the expression of the pluripotency marker Oct4 was previously suggested by Faherty *et al.*[11] To quantify this effect in our device, we recorded daily fluorescence images of all microwells and evaluated the green fluorescent signal of GFP due to the expression of the Oct4 cell marker. We used the IMAGEJ software to measure the fluorescence intensity in each well, averaged it across all wells and normalized that data by the maximum signal intensity obtained on-chip. In the gradient experiment, we supplied different concentrations of LIF to the captured cells. We introduced pure culture medium (without LIF) and LIF-containing medium through inlets 1 and 2, with both solutions flowing at 200 μl/h. We again imaged the cells daily in phase contrast and fluorescence and measured the fluorescence signal as detailed above.

The control experiments—with varying static concentrations of LIF—were conducted on microwell platforms designed for static culture. The individual platforms consisted of a microwell array laser ablated onto a polyester layer, as described elsewhere,[50] and glued onto a blank PDMS slab. Each microwell platform was kept inside a separate well on a 6-well plate and stored in a cell culture incubator. The culture medium was replenished daily. The imaging and data analysis were conducted in the same way as for the continuously perfused chips, with the average GFP signal measured across 200 microwells. After the 5-day cell culture, the medium was aspirated in the static devices, and the devices transferred to new polystyrene dishes and washed with PBS. The viability assay was added to the microwell platforms via pipetting. Otherwise, the same procedure was followed as in the continuous perfusion experiment.

Statistical analysis

Statistical significance was determined by one-way analysis of variance (ANOVA, Tukey's Range Test). For all statistical tests, the level of significance was set to $p < 0.05$.

RESULTS AND DISCUSSION

Device fabrication and operation

Initially, when filling the device with an aqueous solution, the air bubbles captured in the hydrophobic device were difficult to remove, as they were pinned to the microchannel walls. High flow rates (above 400 μl/h) were required to compress the air into the PDMS layer, which in turn led to device delamination. To remedy this problem, we temporarily rendered the polyester and PDMS

This article is copyrighted as indicated in the article. Reuse of AIP content is subject to the terms at: http://scitation.aip.org/termsconditions. Downloaded to IP: 18.7.29.240 On: Wed, 19 Aug 2015 20:51:52

walls of the microchannels hydrophilic by treating them with oxygen plasma. This enabled wetting of the channel walls with the aqueous solution and facilitated removal of the gas bubbles. (See supplementary material Figure S-1 for contact angle measurements on polyester prior to and after plasma treatment.)[51,54] All laser ablated features had uniform dimensions and few defects, which was important for the removal of air bubbles, subsequent seeding of cells and generation of stable concentration gradients.

Numerical analysis

We used COMSOL to generate a plot of FITC concentration in water inside the main channel. Specifically, the dye concentration was calculated in the direction transverse to the flow and at different positions inside the main channel, downstream of the two inlets. Adding lateral channel branches (Figure 1) resulted in a redistribution of the fluids, which enabled full mixing of the clear and dyed solutions inside a relatively short main channel (23 mm). This allowed us to retain the small footprint of our microfluidic device. Furthermore, we generated non-linear concentration gradient profiles inside the channel branches for rhodamine B and FITC, for three main channel widths (800, 1000, 1200 μm) and for three different channel branch widths (500, 800, 1000 μm). This information was used to determine the optimal channel widths for our experiments, namely 800 μm for the channel branches and 1 mm for the main channel. These dimensions were small enough to allow for wide concentration gradients, but large enough to generate smooth features during laser printing of the polyester layer.

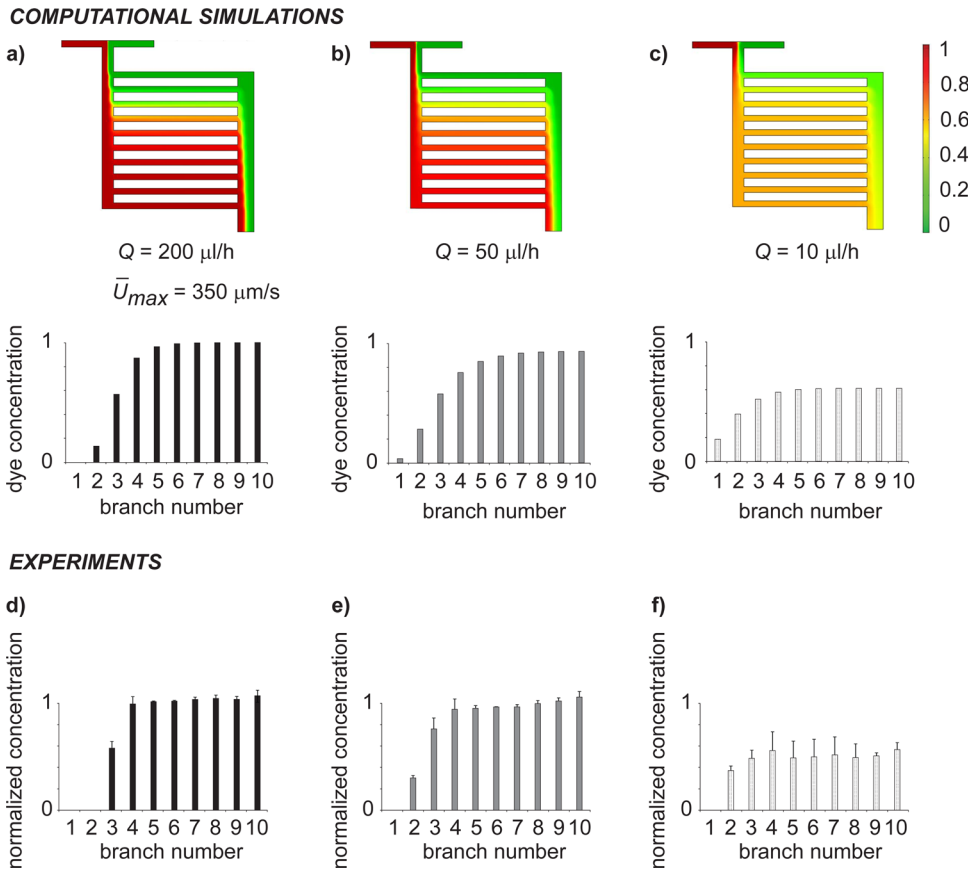

FIG. 2. Comparison between results of the COMSOL simulation ((a)–(c)) and the experimental setup ((d)–(f)) showing the normalized FITC concentration profiles for different input flow rates: 200 μl/h, 50 μl/h, 10 μl/h (per stream). These values translate to a maximum average flow velocity of 350 μm/s per channel. A top view representation of the microfluidic device is also shown in (a)–(c), indicating the normalized concentration of FITC in each branch for the respective flow rates.

This article is copyrighted as indicated in the article. Reuse of AIP content is subject to the terms at: http://scitation.aip.org/termsconditions. Downloaded to IP: 18.7.29.240 On: Wed, 19 Aug 2015 20:51:52

Our numerical results indicated that the concentration gradient profiles (Figures 2(a)–2(c)) could be fit with an exponential curve at low flow rates (e.g., 10 μl/h). At higher flow rates ($Q \geq 50$ μl/h), however, the profiles had sigmoidal fits, similar to our previous results. The curve fits were generated using Origin 8.0 (Origin Lab, Northampton, MA) and are included in the supplementary material, Figure S-2 (for FITC).[51]

Our experimental observations indicated that the cells could not be captured during cell loading at $Q_{cell} = 7200$ μl/h. This result informed our decision to interrupt the flow and allow the cells to settle to the bottom of the wells. Once the cells were captured in this way, we re-established the flow of medium through the device ($Q = 300$ μl/h per stream). To calculate the shear stresses acting on cells inside a microwell, we created a CFD-ACE+ three-dimensional model of the region around a single microwell. The maximum strain rate experienced by the cells in this configuration was 1.5 s^{-1}, corresponding to a shear stress of 117 dynes cm^{-2} or 1.17×10^{-3} Pa (Figure 3(a)). A similarly low shear stress was calculated when a large cell aggregate was modeled inside the microwell (Figure 3(b)). According to literature results,[57,58] a shear stress on the order of 10^{-3} Pa would not cause cell damage or stem cell differentiation, allowing us to utilize the chosen parameters in our experiments.

Gradient generation

Figures 2(d)–2(f) show the experimental results of the FITC concentration gradient generation, at three different flow rates (10 μl/h, 50 μl/h, and 200 μl/h, from right to left). The averages of 10 wells per branch and n = 3 devices are displayed. The error bars indicate the standard deviation. The flow was more stable at higher flow rates than at lower ones, which was manifested in smaller experimental errors. Nonetheless, our experimental results corresponded well with our numerical predictions of the concentration gradient profiles. Interestingly, the gradient profiles at 50 μl/h and 200 μl/h were similar, both in our simulations and in experiments. We suggest that this was due to the relatively wide main channel (1 mm), as previous experiments

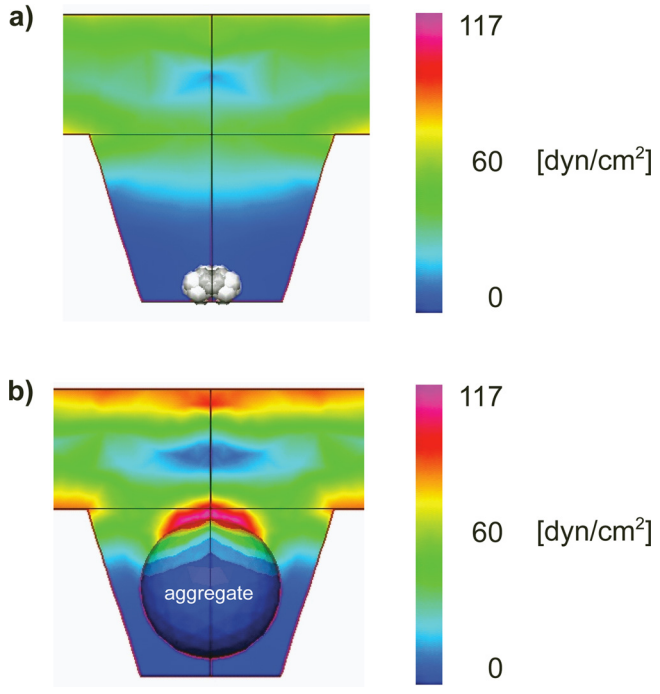

FIG. 3. Colorimetric map indicating the shear stress acting on the cells after the initial cell loading (a) and later in the culture, when the cell aggregate almost completely filled the microwell (b). Both images show the cross-section of a microwell. The direction of flow is from left to right. The total applied flow rate in the model was 400 μl/h. This translates to an average velocity per channel branch of 350 μm/s.

This article is copyrighted as indicated in the article. Reuse of AIP content is subject to the terms at: http://scitation.aip.org/termsconditions. Downloaded to IP: 18.7.29.240 On: Wed, 19 Aug 2015 20:51:52

utilizing a narrower channel (200 μm) allowed for a faster diffusion-based mixing of the small FITC molecules and so a more pronounced difference between gradient profiles.[26] Thus, we decided to adopt the higher flow rate of 200 μl/h for our subsequent experiments, because this rate allowed for any flow instabilities to pass through the device faster than at lower flow rates. Such instabilities could potentially occur as a result of errors in pump operation or motion of the thin-walled polytetrafluoroethylene (PTFE) tubing, especially when the device was moved for daily imaging. Furthermore, we expected that the gradients would also be more stable for larger molecules, which diffuse more slowly, such as LIF (22 kDa). A comparison between concentration gradients of rhodamine B and LIF is shown in the supplementary material, Figure S-3.[51] Here, we estimated the diffusion constant of LIF to be 1×10^{-10} m^2/s, similar to other molecules of the same size.[59]

Cell loading, aggregate formation, and viability

The cell loading method described previously ensured that most of the 100 microwells ($86 \pm 5\%$) in each of the three devices were filled with a large number of cells and that the cell distribution across the wells was uniform. This was verified by visual inspection of the device. Our observation was in line with the prediction of the fluid dynamics simulation by Kang *et al.*[60] that the relatively uniform shear stress in concave microwells enables more uniform cell loading than inside cylindrical microwells. The location of the empty microwells varied from device to device, suggesting the possibility that the manual loading method, rather than the device structure was responsible for the empty sites. The continuously perfused cells began forming aggregates within a few hours after seeding.[26] The cell aggregates grew steadily until day 5, when many were large enough to completely fill the microwells. This information is summarized in Figures 4(b) and 4(c). Representative phase contrast images of a subset of microwells are shown in Figure 4(a) at days 1, 3, and 5 of culture, at two different magnifications (2× and 10×), and, in the supplementary material, Figure S-4[51] at days 1, 3, and 5 of culture, at 4×, and Figure S-5[51] at day 5, at 20×. On the last day of culture, we conducted a viability

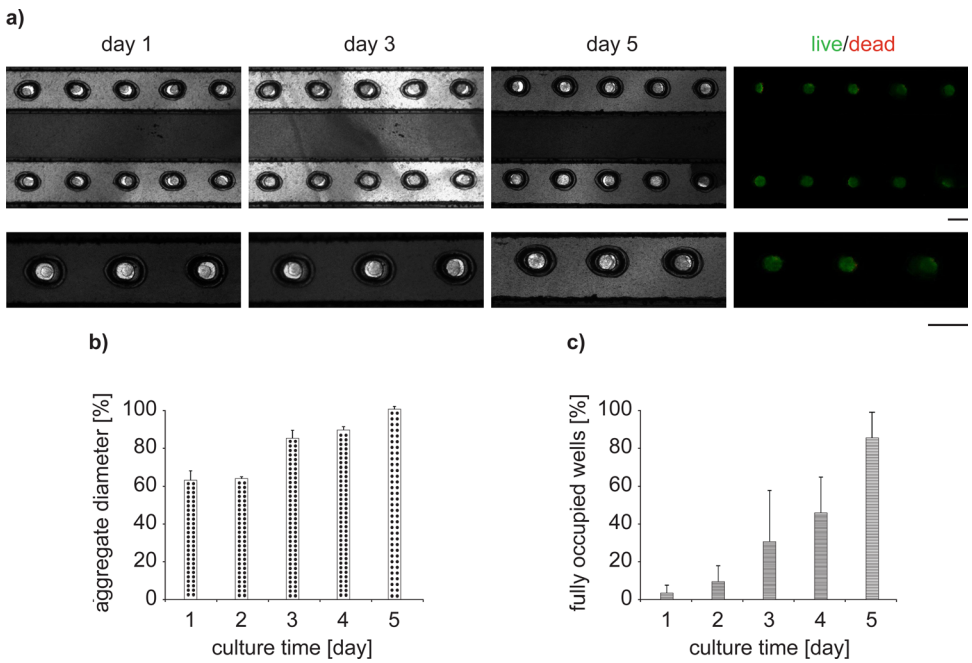

FIG. 4. (a) Representative phase contrast and live/dead fluorescence images of mESC aggregates growing inside the microwells over the course of 5 days (at 2× and 10× magnification). Live cells were labeled green, while dead cells were labeled red. (b) Fraction of microwell area occupied by cell aggregates and (c) fraction of fully occupied wells as a function of culture time. Scale bars: 400 μm.

This article is copyrighted as indicated in the article. Reuse of AIP content is subject to the terms at: http://scitation.aip.org/termsconditions. Downloaded to IP: 18.7.29.240 On: Wed, 19 Aug 2015 20:51:52

test. Live cells stained green due to the continued expression of GFP, when LIF stimulated Oct4 expression. Dead cells stained red after binding of ethidium homodimer to the DNA of membrane-compromised cells. The scarcity of red fluorescent signal indicated that few cells had died (Figure 4(a), right most panel). A mechanism for extraction of the cell aggregates from the individual microwells was not in place at this point, limiting our cell analysis in visual observation.

These results match qualitatively the findings from previous research,[50] where mESCs were cultured under static conditions. However, in perfusion culture, the formed cell aggregates filled the microwells almost completely by day 5, which was 4 days earlier than in static culture. While we did not explore the cause of this result experimentally, we suggest the following possible factors. Due to the advanced and well-controlled cell loading method the number of cells per microwell was on average higher on the polyester μ-well chip than on the static culture platform, resulting in earlier formation (culture day 1 vs. day 3) of cell aggregates. Furthermore, the continuous provision of fresh culture medium and removal of metabolic waste inside the microfluidic device could potentially act to increase the cell activity and, ultimately, the initial rate of cell proliferation. Last, in the static culture case the daily exchange of medium via aspiration and pipetting could have resulted in removal of unbound cells from the microwells, thereby reducing the number of cells available for inclusion into a larger unit.

Stem cell pluripotency

We evaluated the loss of mESC pluripotency by quantifying the expression of GFP, caused by the continued production of Oct4 marker. Here we only considered microwells that contained a single cell aggregate. We quantified the GFP signal for the case of a LIF concentration gradient (0–1000 U/ml) and a constant LIF concentration (1000 U/ml) across all channel branches. In both cases, the medium was perfused continuously to achieve dynamic culture conditions. When the same concentration of LIF was delivered to all channel branches, then all formed cell aggregates expressed the same amount of GFP, as expected. Therefore, we concluded that the expression of Oct4 was also equal across all microwells. An applied LIF gradient, however, affected the GFP expression (and presumably Oct4) across the different channel branches. In our previous work,[25] we could generate up to ten different conditions using the same gradient generator structure, however, the precise gradient shape and number of conditions depends on the diffusion constant of the solute as well as the channel dimensions. In the present study, we chose to generate four distinct LIF concentrations using the gradient generator. Figure 5 shows the results of this experiment. Phase contrast and fluorescence images of microwells in branches 1 (no presence of LIF) and 10 (maximum concentration of LIF) were compared on days 1 and 5 of culture (Figures 5(a)–5(d)). The LIF concentration gradient across the 10 channel branches was predicted numerically (Figure 5(e)). It resulted in GFP (and thus Oct4) expression gradients as shown in Figures 5(f) and 5(g), on cell culture days 1 and 5. By day 5, a significant difference in GFP expression across the different channels was observed.

As a control, we measured the Oct4 expression in mESCs in static culture experiments. Again, we only considered microwells containing single cell aggregates. In these experiments different LIF concentrations were manually prepared and their effect on the mESCs tested. To streamline this experiment and reduce the consumption of LIF, we tested the effects of only four LIF concentrations: 0, 300, 750, and 1000 U/ml. The number of analyzed wells was 200. Our choice of these values was based on the results from the continuous perfusion experiments. Namely, we hypothesized that a similar relationship between those LIF concentrations and fluorescence intensity would be observed in the static culture. Figure 5(g) shows the fluorescence images of statically cultured mESC aggregates, as well as live/dead images recorded on the last day of culture. The corresponding values of the fluorescence intensity on culture days 1 and 5 are shown in Figure 5(h). The gradual reduction in fluorescence in absence of LIF was comparable to branches 1 and 2 in the dynamic culture. However, there was no evidence of a significant variation in fluorescence at all other LIF concentrations in the control experiment. This comparison of dynamic and static cultures suggest that the expression of Oct4 and GFP was

This article is copyrighted as indicated in the article. Reuse of AIP content is subject to the terms at: http://scitation.aip.org/termsconditions. Downloaded to IP: 18.7.29.240 On: Wed, 19 Aug 2015 20:51:52

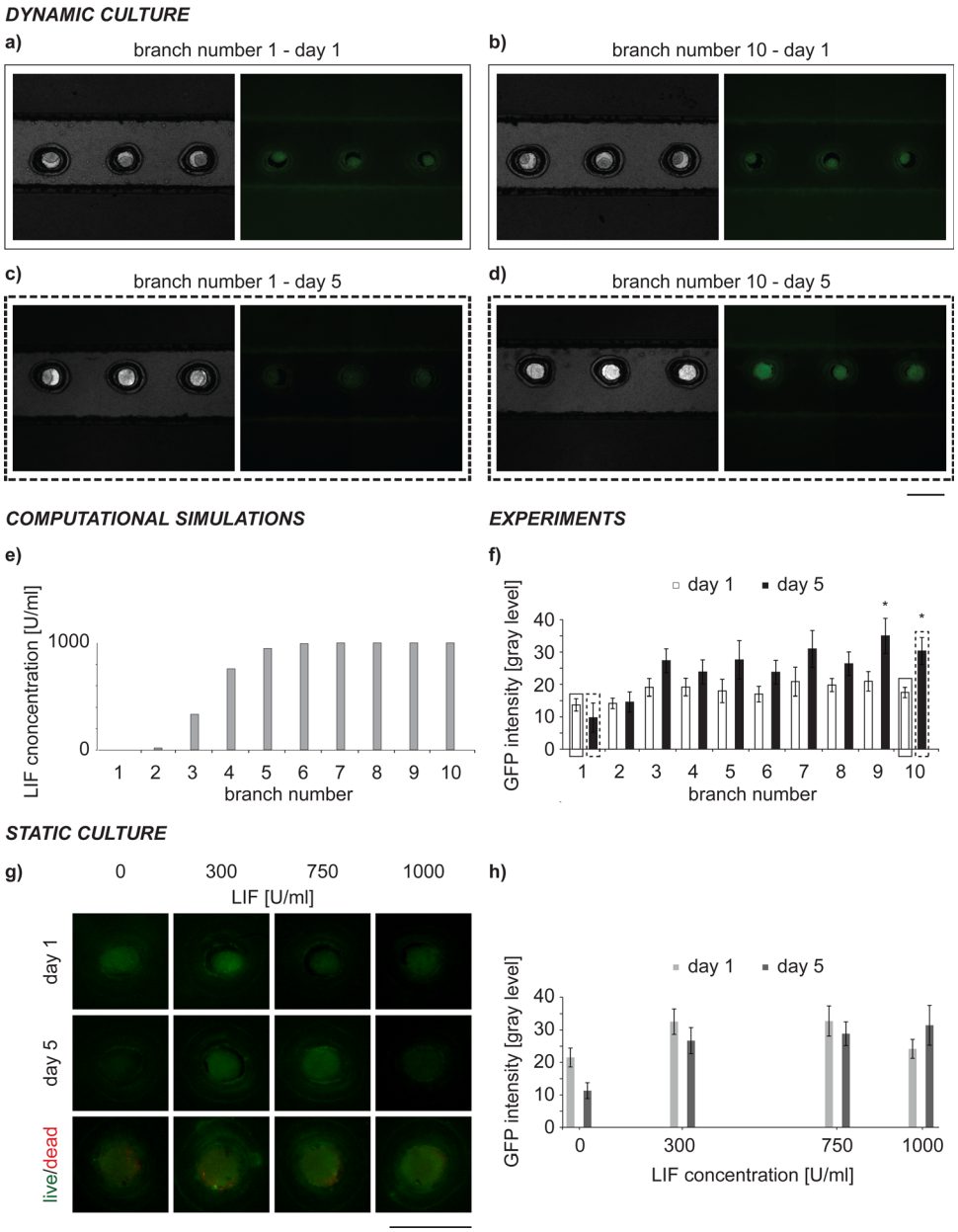

FIG. 5. Expression of GFP driven by Oct4 promoter ((a)–(d)) in representative microwells from branches 1 (no LIF) and 10 (1000 U/ml LIF), on days 1 and 5 of culture. The numerically predicted LIF concentration gradient is shown in (e), giving rise to a gradient in GFP (and hence Oct4) expression across the ten branches on days 1 and 5 (f). Images from the control experiment (static culture) are shown in (g), and the corresponding data in (h), relating the GFP intensity to the predicted LIF concentration. Scale bars: 400 μm.

qualitatively similar on the static and dynamic platforms, but the control over the pluripotency of mESCs was more efficient when LIF-containing culture medium was continuously supplied.

The work published by Faherty *et al.*,[11] similarly, shows that the addition of 1000 U/ml LIF to the culture medium induced the continued maximum production of Oct4 in mESCs, while the lack of LIF allowed the Oct4 expression to subside with cell aggregate growth. There are, however, two distinguishing factors between this study and our on-chip experiment: the cells used by Faherty belonged to a different cell line (IOUD2), and they were cultured on a gelatin-coated well-plate under static conditions. These geometric and flow constraints, as well as the presence of gelatin could potentially affect the cell activity and production of Oct4.

This article is copyrighted as indicated in the article. Reuse of AIP content is subject to the terms at: http://scitation.aip.org/termsconditions. Downloaded to IP: 18.7.29.240 On: Wed, 19 Aug 2015 20:51:52

Namely, when cultured for 6 days without LIF, the cells in Faherty's work were still expressing very high Oct4 amounts. For comparison, we measured already after 5 days a 50% reduction in maximum GFP expression (hence, in Oct4) on our static microwell platform. On our polyester μ-assay chip that percentage was reduced to below 30%. These data suggest that the GFP/Oct4 expression and the conditions of culture, e.g., flow, might be correlated. However, further studies could provide more insight into this issue.

At this point, we note that the weak fluorescence signal in cells starved of LIF could include an autofluorescence component. To determine the amount of autofluorescence, we could in the future culture the cells for an extended amount of time, namely until the signal intensity of cells starved of LIF becomes independent of culture time.

CONCLUSION

An experiment focusing on stem cell pluripotency supported by a numerical study demonstrated that the polyester μ-assay chip offered control over the generation and distribution of a chemical concentration gradient. Our device was shown to carry several key advantages. It was fabricated by laser-ablation of a polyester film, which is a simple, bench-top, and low-cost fabrication method and suitable for development of microscale devices. Since this is a direct-write method, it is also amenable to fast design changes. Next, the use of the non-linear gradient generator as shown here allowed us to dispense with complex microscale elements for mixing and distribution of liquids, thereby reducing the size of the chip. At the same time, however, the chip offered a concentration gradient generator coupled with a continuous perfusion system and a microwell array for cell storage and culture. The only piece of external equipment needed was a single syringe pump for continuous culture perfusion, such that the device could be operated by personnel with little technical skill. In addition, the use of a dynamic perfusion system meant that human work was only required for the experimental set-up. Although the microwells were monitored daily, the imaging could be automated by adding a mini-microscope or a lensless CMOS imaging platform in the incubator.[61] Most importantly, however, the device material did not require any additional surface treatment and did not show any deleterious effects on stem cell proliferation and viability, enabling further, more advanced differentiation studies. The cells were contained inside a closed, sterilized device, reducing the likelihood of contamination.

With respect to its precursor, the open static culture microwell platform, the polyester μ-assay chip was more efficient. Namely, the cell seeding was denser and more uniform than on the open platform, resulting in a large proportion of aggregate-containing wells early in the culture period. Finally, our data suggest that the dynamic flow conditions inside the microfluidic device potentially increased the mESC sensitivity to chemicals such as LIF. Additional studies are required to confirm this hypothesis, however, a high sensitivity to chemicals would decrease the experimental time, reduce the amount of reagents used for cell screening and ultimately increase the value of our device even further.

In the future, we envision that the Polyester μ-well chip may be modified with a high-precision laser engraver to enable patterning on a 10 μm scale and, in consequence, investigations of single cell, cell-cell and cell-substrate interactions, while taking advantage of dynamic analysis and full automation. The PDMS bottom could also be selectively functionalized with fibronectin or other proteins to control cell adhesion. In addition, a second gradient structure could be placed perpendicularly to the current network, similar to our previous work,[56] giving rise to a 2D, combinatorial mixture of chemicals and the simultaneous testing of many more conditions. Here, any of the structures supporting passive or active concentration gradients, like discussed in the introduction, could be included. The stacking of microwells and fluidic channels on three or more layers in the z-direction[27] could then lead to the inclusion of additional microwells and so increase the throughput capabilities of the device. Alternatively, to further simplify the device, the syringe pump could be replaced by a gravity-driven micro-pump.[62] We also plan to include a mechanism for extraction of the cell aggregates in order to extend the currently enabled screening studies on the Polyester μ-well chip to experiments focused on

This article is copyrighted as indicated in the article. Reuse of AIP content is subject to the terms at: http://scitation.aip.org/termsconditions. Downloaded to IP: 18.7.29.240 On: Wed, 19 Aug 2015 20:51:52

stem cell biology. Such a mechanism could be based on peeling off the PDMS layer and looping the cell aggregates out with a metal wire, as is commonly done with protein crystals,[63,64] or applying negative pressure to one particular channel to suck out all aggregates cultured at the same experimental condition. Either approach would enable subsequent cell studies including fluorescence activated cell sorting and polymerase chain reaction (PCR).

ACKNOWLEDGMENTS

We gratefully acknowledge the following funding support: Fondazione Fratelli Agostino and Enrico Rocca through the Progetto Rocca (F.P.); Politecnico di Torino Scholarship (M.A. and A.P.); NIH Grant Nos. HL092836, EB012597, and HL099073, and the Office of Naval Research (A.K.). F.P., A.K., Š.S., and D.D. conceived of the study; F.P. and Š.S. developed the microfluidic device and designed the experiments; F.P., Š.S., M.A., and S.M. conducted experiments; A.P. and S.B.K. conducted numerical and analytical calculations; F.P., Š.S., M.A., A.P., and S.M. analyzed the data.

[1]S. Levenberg, J. S. Golub, M. Amit, J. Itskovitz-Eldor, and R. Langer, Proc. Natl. Acad. Sci. U.S.A. **99**, 4391 (2002).
[2]J. Oswald, S. Boxberger, B. Jorgensen, S. Feldmann, G. Ehninger, M. Bornhauser, and C. Werner, Stem Cells **22**, 377 (2004).
[3]T. Kawai, T. Takahashi, M. Esaki, H. Ushikoshi, S. Nagano, H. Fujiwara, and K. Kosai, Circ. J. **68**, 691 (2004).
[4]I. Kehat, D. Kenyagin-Karsenti, M. Snir, H. Segev, M. Amit, A. Gepstein, E. Livne, O. Binah, J. Itskovitz-Eldor, and L. Gepstein, J. Clin. Invest. **108**, 407 (2001).
[5]C. Mummery, D. Ward, C. E. van den Brink, S. D. Bird, P. A. Doevendans, T. Opthof, A. Brutel de la Riviere, L. Tertoolen, M. van der Heyden, and M. Pera, J. Anat. **200**, 233 (2002).
[6]T. Takahashi, B. Lord, P. C. Schulze, R. M. Fryer, S. S. Sarang, S. R. Gullans, and R. T. Lee, Circulation **107**, 1912 (2003).
[7]H. Baharvand, S. M. Hashemi, S. Kazemi Ashtiani, and A. Farrokhi, Int. J. Dev. Biol. **50**, 645 (2006).
[8]T. Hamazaki, Y. Iiboshi, M. Oka, P. J. Papst, A. M. Meacham, L. I. Zon, and N. Terada, FEBS Lett. **497**, 15 (2001).
[9]T. Ishii, K. Yasuchika, H. Fujii, T. Hoppo, S. Baba, M. Naito, T. Machimoto, N. Kamo, H. Suemori, N. Nakatsuji, and I. Ikai, Exp. Cell Res. **309**, 68 (2005).
[10]I. Barkefors, S. Le Jan, L. Jakobsson, E. Hejll, G. Carlson, H. Johansson, J. Jarvius, J. W. Park, N. Li Jeon, and J. Kreuger, J. Biol. Chem. **283**, 13905 (2008).
[11]S. Faherty, M. T. Kane, and L. R. Quinlan, In Vitro Cell. Dev. Biol.: Anim. **41**, 356 (2005).
[12]B. G. Chung, L. A. Flanagan, S. W. Rhee, P. H. Schwartz, A. P. Lee, E. S. Monuki, and N. L. Jeon, Lab Chip **5**, 401 (2005).
[13]L. M. Przybyla and J. Voldman, Proc. Natl. Acad. Sci. U.S.A. **109**, 835 (2012).
[14]A. Khademhosseini, R. Langer, J. Borenstein, and J. P. Vacanti, Proc. Natl. Acad. Sci. U.S.A. **103**, 2480 (2006).
[15]K. Gupta, D. H. Kim, D. Ellison, C. Smith, A. Kundu, J. Tuan, K. Y. Suh, and A. Levchenko, Lab Chip **10**, 2019 (2010).
[16]H. W. Wu, C. C. Lin, S. M. Hwang, and G. B. Lee, presented at the *14th International Conference on Miniaturized Systems for Chemistry and Life Sciences, Groningen, The Netherlands, Proceedings of MicroTAS 2010* (MicroTAS, 2010), p. 13.
[17]D. van Noort, S. M. Ong, C. Zhang, S. Zhang, T. Arooz, and H. Yu, Biotechnol. Prog. **25**, 52 (2009).
[18]C. Yi, C. W. Li, S. Ji, and M. Yang, Anal. Chim. Acta **560**, 1 (2006).
[19]E. W. Young and D. J. Beebe, Chem. Soc. Rev. **39**, 1036 (2010).
[20]A. Webster, J. Greenman, and S. J. Haswella, J. Chem. Technol. Biotechnol. **86**, 10 (2011).
[21]M. S. Munson and P. Yager, presented at the *7th International Conference on Miniaturized Chemical and Biochemical Analysis Systems, Squaw Valley, CA, USA, Proceedings of MicroTAS 2003* (MicroTAS, 2003), p. 495.
[22]N. L. Jeon, S. K. Dertinger, D. T. Chiu, I. S. Choi, A. D. Stroock, and G. M. Whitesides, Langmuir **16**, 8311 (2000).
[23]D. Irimia, D. A. Geba, and M. Toner, Anal. Chem. **78**, 3472 (2006).
[24]L. Kim, M. D. Vahey, H. Y. Lee, and J. Voldman, Lab Chip **6**, 394 (2006).
[25]Š. Selimović, W. Y. Sim, S. B. Kim, Y.-H. Jang, W. G. Lee, M. Khabiry, H. Bae, S. Jambovane, J. W. Hong, and A. Khademhosseini, Anal. Chem. **83**, 2020 (2011).
[26]L. F. Barros, T. Kanaseki, R. Sabirov, S. Morishima, J. Castro, C. X. Bittner, E. Maeno, Y. Ando-Akatsuka, and Y. Okada, Cell Death Differ. **10**, 687 (2003).
[27]C. Neils, Z. Tyree, B. Finlayson, and A. Folch, Lab Chip **4**, 342 (2004).
[28]H. P. Chou, M. A. Unger, and S. R. Quake, Biomed. Microdevices **3**, 323 (2001).
[29]H. Suzuki, C. M. Ho, and N. Kasagi, J. Microelectromech. Syst. **13**, 779 (2004).
[30]R. H. Liu, M. A. Stremler, K. V. Sharp, M. G. Olsen, J. G. Santiago, R. J. Adrian, H. Aref, and D. J. Beebe, J. Microelectromech. Syst. **9**, 190 (2000).
[31]X. Jiang, Q. Xu, S. K. Dertinger, A. D. Stroock, T. M. Fu, and G. M. Whitesides, Anal. Chem. **77**, 2338 (2005).
[32]M. S. Williams, K. J. Longmuir, and P. Yager, Lab Chip **8**, 1121 (2008).
[33]A. D. Stroock, S. K. W. Dertinger, A. Ajdari, I. Mezic, H. A. Stone, and G. M. Whitesides, Science **25**, 647 (2002).
[34]S. Kim, H. J. Kim, and N. L. Jeon, Integr. Biol. **2**, 584 (2010).
[35]K. Norrby and L. Franzen, In Vitro Cell. Dev. Biol.: Plant **16**, 31 (1980).
[36]D. B. Mountcastle, E. Freire, and R. L. Biltonen, Biopolymers **15**, 355 (1976).
[37]J. Y. Park, C. M. Hwang, S. H. Lee, and S. H. Lee, Lab Chip **7**, 1673 (2007).
[38]J. El-Ali, P. K. Sorger, and K. F. Jensen, Nature **442**, 403 (2006).

This article is copyrighted as indicated in the article. Reuse of AIP content is subject to the terms at: http://scitation.aip.org/termsconditions. Downloaded to IP: 18.7.29.240 On: Wed, 19 Aug 2015 20:51:52

[39]B. Mosadegh, M. Agarwal, H. Tavana, T. Bersano-Begey, Y. Torisawa, M. Morell, M. J. Wyatt, K. S. O'Shea, K. F. Barald, and S. Takayama, Lab Chip **10**, 2959 (2010).
[40]R. Gomez-Sjoberg, A. A. Leyrat, D. M. Pirone, C. S. Chen, and S. R. Quake, Anal. Chem. **79**, 8557 (2007).
[41]C. Kim, K. S. Lee, J. H. Bang, Y. E. Kim, M. C. Kim, K. W. Oh, S. H. Lee, and J. Y. Kang, Lab Chip **11**, 874 (2011).
[42]S. Lindstrom, K. Mori, T. Ohashi, and H. Andersson-Svahn, Electrophoresis **30**, 4166 (2009).
[43]M. Khoury, A. Bransky, N. Korin, L. C. Konak, G. Enikolopov, I. Tzchori, and S. Levenberg, Biomed. Microdevices **12**, 1001 (2010).
[44]Y. Y. Choi, B. G. Chung, D. H. Lee, A. Khademhosseini, J. H. Kim, and S. H. Lee, Biomaterials **31**, 4296 (2010).
[45]Y. Sakai, Y. Yoshiura, and K. Nakazawa, J. Biosci. Bioeng. **111**, 85 (2011).
[46]Y. Xu, F. Xie, T. Qiu, L. Xie, W. Xing, and J. Cheng, Biomicrofluidics **6**, 16504 (2012).
[47]L. Liu, C. Luo, X. Ni, L. Wang, K. Yamauchi, S. M. Nomura, N. Nakatsuji, and Y. Chen, Biomed. Microdevices **12**, 505 (2010).
[48]Y. C. Toh, C. Zhang, J. Zhang, Y. M. Khong, S. Chang, V. D. Samper, D. van Noort, D. W. Hutmacher, and H. Yu, Lab Chip **7**, 302 (2007).
[49]Y. C. Toh, T. C. Lim, D. Tai, G. Xiao, D. van Noort, and H. Yu, Lab Chip **9**, 2026 (2009).
[50]Š. Selimović, F. Piraino, H. Bae, M. Rasponi, A. Redaelli, and A. Khademhosseini, Lab Chip **11**, 2325 (2011).
[51]See figures in the supplementary material at http://dx.doi.org/10.1063/1.4766300 for details.
[52]G. C. Randall and P. S. Doyle, Proc. Natl. Acad. Sci. U.S.A. **102**, 10813 (2005).
[53]S. C. Finkner and J. E. Gilley, Appl. Eng. Agric. **2**, 104 (1986). Available at http://naldc.nal.usda.gov/download/17376/PDF.
[54]K. Ziolkowska, A. Stelmachowska, R. Kwapiszewski, M. Chudy, A. Dybko, and Z. Brzozka, "Long-term three-dimensional cell culture and anticancer drug activity evaluation in a microfluidic chip," Biosens. Bioelectron. (in press).
[55]A. Khademhosseini, J. Yeh, G. Eng, J. Karp, H. Kaji, J. Borenstein, O. C. Farokhzad, and R. Langer, Lab Chip **5**, 1380 (2005).
[56]Y. H. Jang, C. H. Kwon, S. B. Kim, S. Selimovic, W. Y. Sim, H. Bae, and A. Khademhosseini, Biotechnol. J. **6**, 156 (2011).
[57]H. Wang, G. M. Riha, S. Yan, M. Li, H. Chan, H. Yang, Q. Yao, and C. Chen, Arterioscler., Thromb., Vasc. Biol. **25**, 1817 (2005).
[58]Y. C. Toh and J. Voldman, FASEB J. **25**, 1208 (2011).
[59]F. Ferrage, M. Zoonens, D. E. Warschawski, J. L. Popot, and G. Bodenhausen, J. Am. Chem. Soc. **125**, 2541 (2003).
[60]E. Kang, Y. Y. Choi, Y. Jun, B. G. Chung, and S.-H. Lee, Lab Chip **10**, 2651 (2010).
[61]S. B. Kim, H. Bae, J. M. Cha, S. J. Moon, M. R. Dokmeci, D. M. Cropek, and A. Khademhosseini, Lab Chip **11**, 1801 (2011).
[62]Z. R. Xu, C. G. Yang, C. H. Liu, Z. Zhou, J. Fang, and J. H. Wang, Talanta **80**, 1088 (2010).
[63]T.-Y. Teng, J. Appl. Cryst. **23**, 387 (1990).
[64]D. W. Rodgers, Methods Enzymol. **276**, 183 (1997).

This article is copyrighted as indicated in the article. Reuse of AIP content is subject to the terms at: http://scitation.aip.org/termsconditions. Downloaded to IP: 18.7.29.240 On: Wed, 19 Aug 2015 20:51:52